Lecture Series

Modern Methods in Heterogeneous Catalysis

Measurement and Analysis of Kinetic Data

Raimund Horn

Fritz-Haber-Institute of the MPG

Department of Inorganic Chemistry

Faradayweg 4-6

14195 Berlin

Phone: 030 - 8413 - 4420

E-Mail: horn_r@fhi-berlin.mpg.de

07.12.2007

Contents

1 Motivation of Kinetic Measurements

1.1 Kinetic Measurements for Design Purposes

- design of chemical reactors: laboratory → pilot plant → plant
- empirical kinetic expression e.g. $r = k \cdot \prod\limits_i c_i^{\nu_i}$
- quality control in catalyst production
- comparison of different catalyst brands
- catalyst deactivation studies

1.2 Kinetic Measurements for Mechanistic Studies

- a rate law derived from a proposed reaction mechanism (e.g. from literature data, reaction specific experiments, theoretical calculations) has to be conform with the measured kinetic data but a reaction mechanism can not be derived from kinetic data alone (additional spectroscopic experiments, calculations etc. necessary)
- general form of a rate law: $r = f(c_1, c_2, ..., c_i, T, N_T, k_1, k_2, ..., k_i, K_1, K_2, ..., K_i)$
- conformity is verified by comparing numerical predictions with experimental rate data by means of statistical methods
- conformity does not prove the proposed mechanism as true because different mechanisms can predict the same rate data equally well, however, nonconformity disproves a mechanism
- fit of rate law to rate data can provide kinetic parameters

2 Elementary Concepts

2.1 Rate of (Heterogeneous Catalytic) Reactions

2.1.1 Single Stoichiometric Reaction

- the rate of a chemical reaction (only in connection with defining equation) is defined as

$$r = \dot{\xi} = \frac{1}{\nu_i} \frac{dn_i}{dt} \quad [r] = \frac{mol}{s} \tag{1}$$

- example: ammonia synthesis

$$N_2 + 3H_2 \rightarrow 2NH_3 \tag{2}$$

introduction of extent of reaction ξ, $[\xi] = mol$:

$$n_{N_2}(t) = n_{N_2}(0) - 1 \cdot \xi(t) \tag{3}$$

$$n_{H_2}(t) = n_{H_2}(0) - 3 \cdot \xi(t) \tag{4}$$

$$n_{NH_3}(t) = n_{NH_3}(0) + 2 \cdot \xi(t) \tag{5}$$

rate of N_2 consumption:

$$\frac{dn_{N_2}}{dt} = -1 \cdot \frac{d\xi}{dt} = -1 \cdot \dot{\xi} \tag{6}$$

rate of H_2 consumption:

$$\frac{dn_{H_2}}{dt} = -3 \cdot \frac{d\xi}{dt} = -3 \cdot \dot{\xi} \tag{7}$$

rate of NH_3 production:

$$\frac{dn_{NH_3}}{dt} = +2 \cdot \frac{d\xi}{dt} = +2 \cdot \dot{\xi} \tag{8}$$

rate of reaction $\dot{\xi}$ in mol/s

$$r = \dot{\xi} = \frac{1}{-1} \frac{dn_{N_2}}{dt} = \frac{1}{-3} \frac{dn_{H_2}}{dt} = \frac{1}{+2} \frac{dn_{NH_3}}{dt} \tag{9}$$

- r is an extensive quantity and as such dependent on the size of the reaction system

- it is more practical to make r independent of the size of the reaction system (intensive quantity)

- for homogeneous reactions it is common to refer r to the reaction volume

$$r_V = \frac{1}{\nu_i} \frac{dn_i}{V dt} \quad [r_V] = \frac{mol}{m^3 \cdot s} \tag{10}$$

- in heterogeneous catalysis r is typically referred to the catalyst mass $\Rightarrow r_m$

$$r_m = \frac{\dot{\xi}}{m_{cat}} \quad [r_m] = \frac{mol}{kg \cdot s} \tag{11}$$

- even better is to refer r to the surface area of the catalyst $\Rightarrow r_A$ (specify whether A is the total surface area (e.g. from BET) or the surface area of the active component (e.g. from chemisorption measurements))

$$r_A = \frac{\dot{\xi}}{A_{cat}} \quad [r_A] = \frac{mol}{m^2 \cdot s} \tag{12}$$

- most meaningful is the expression of r in terms of a **T**urn **O**ver **F**requency **TOF** in s^{-1}

- with $A =$ catalyst surface area in m^2 and $\Gamma =$ surface site density in $mol\ sites/m^2$

$$TOF = \frac{\dot{\xi}}{\Gamma \cdot A} \tag{13}$$

- ideally, TOF measures a 'site activity' → comparison of catalysts, role of promoters, support effects...

- TOF's are difficult to measure because they require nature and number of active sites to be known (TOF's mostly used for metal catalysts, difficult for oxides)

2.1.2 Multiple Reactions

- if only one stoichiometric reaction describes the changes of all species concentrations (e.g. ammonia synthesis) r can be measured directly by measuring how quickly one involved species is formed or consumed (see Eqn. 1)

- if multiple (j) stoichiometric reactions (so called key reactions) have to be invoked to describe the changes of all species concentrations, r_j can not be determined directly

- example: synthesis gas production by steam reforming of methane (e.g. on Ni catalysts)

$$CH_4 + H_2O \rightarrow CO + 3H_2 \tag{14}$$

$$CO + H_2O \rightarrow CO_2 + H_2 \tag{15}$$

$$CH_4 \rightarrow C + H_2 \tag{16}$$

$$C + H_2O \rightarrow CO + H_2 \tag{17}$$

$$2CO \rightarrow C + CO_2 \tag{18}$$

$$2CH_4 \rightarrow C_2H_6 + H_2 \tag{19}$$

- the reaction rates r_j can not be directly determined from the measurable molar species changes, e.g. $r_{14} \neq dn_{CO}/dt$, because

$$R_{CO} = \frac{dn_{CO}}{dt} = +1 \cdot r_{14} - 1 \cdot r_{15} + 1 \cdot r_{17} - 2 \cdot r_{18} \tag{20}$$

- if all production (consumption) rates of a set of key components [1] can be measured, a linear system of equations like Eqn. 20 results and the r_j can be calculated

- in many cases it is sufficient to work with R_i, the measurable species production (consumption) rate

$$R_i = \sum_j \nu_{ij} r_j \tag{21}$$

2.2 Order and Stoichiometry

- the order of a reaction in the concentration of a certain reactant is given by the best fit between a rate equation and the experimental data

- there is no necessary connection between the kinetic order and the stoichiometry of the reaction

- example $CO + 1/2O_2 \rightarrow CO_2$ on Pd: stoichiometry suggests $n(CO) = 1$ but kinetics suggests $n(CO) = -1$

- stoichiometry and order are rarely equal because a stoichiometric equation is an overall description of a series of elementary steps and but only the slowest step is reflected in a kinetic measurement

- example: $2A + B \rightleftharpoons P$

$$\begin{aligned} Step\,1:\ A + B &\rightleftharpoons (AB) \quad (AB) = K_1AB && (22)\\ Step\,2:\ B + (AB) &\rightleftharpoons (BAB) \quad (BAB) = K_2(AB)B = K_2K_1AB^2 && (23)\\ Step\,3:\ A + (BAB) &\rightleftharpoons P + B && (24)\\ Overall\ :2A + B &\rightleftharpoons P && (25) \end{aligned}$$

- if Step 1 is slowest, $r = k_1 \cdot A \cdot B$; if Step 2 is slowest $r = k_2 \cdot K_1 \cdot A \cdot B^2$; if Step 3 is slowest $r = k_3 \cdot K_2 \cdot K_1 \cdot A^2 \cdot B^2$

3 Kinetic Measurements in the Lab

3.1 General Procedure

- for heterogeneous catalytic reactions, the reaction is usually performed in a catalytic reactor (sometimes batch-, mostly continuous operation)

- it is measured how species concentrations vary with time ($n_i(t)$, $c_i(t)$, $p_i(t)$...)

- in flow systems t is replaced by τ, the contact time between the reactants and the catalyst $\tau = volume\ catalyst\ bed/volumetric\ flow\ rate$

- if the reactor is operated differentially (small conversions $\Delta X_i < 0.1$), the reaction rate can be measured directly

$$r = -\frac{1}{\nu_i}\frac{c_{i,0}dX_i}{dt} \tag{26}$$

and assigned to $c_i = c_{i,0} + \frac{dc_i}{2}$

3.2 Differential Data Analysis

- means that we use the suggested rate law in its differential form, i.e.

$$r = \frac{1}{\nu_i}\frac{dn_i}{dt} = f(c_1, c_2, .c_i., c_n, T) \tag{27}$$

- this requires differential data, i.e., either a direct measurement of the rate r or in case of data like $n_i(t)$, $c_i(t)$, $p_i(t)$ numerical differentiation to yield $\frac{1}{\nu_i}\frac{dn_i}{dt}$, $\frac{1}{\nu_i}\frac{dc_i}{dt}$, $\frac{1}{\nu_i}\frac{dp_i}{dt}$... (see Figure 1)

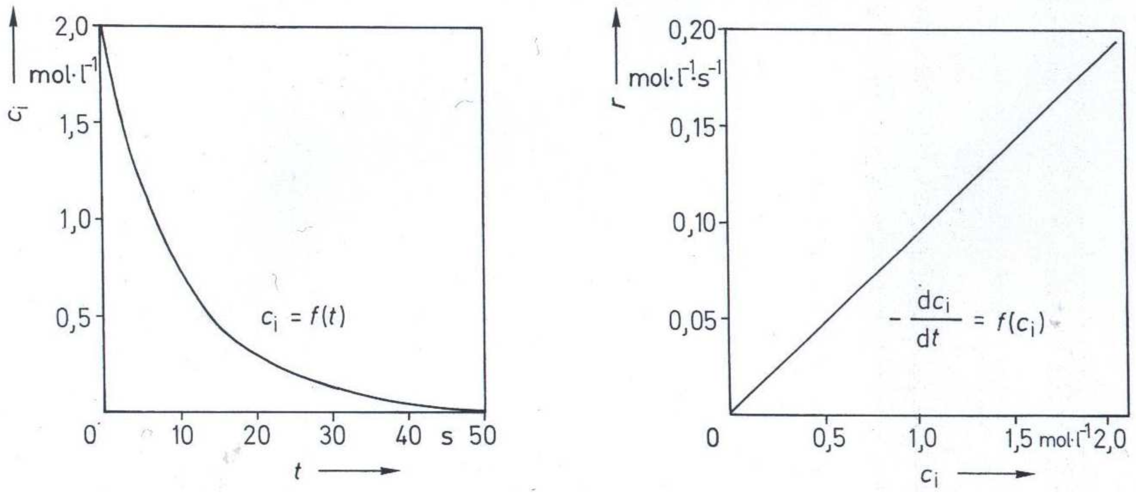

Figure 1: Differential analysis of rate data measured for a first order reaction $r = k \cdot c_i$ (adopted from [1])

- for parameter estimation it is always beneficial to transform the rate law into a linear form because the statistics of linear regression is easy and fully developed

- examples:
  - ◇ $r = k \cdot c_i \Rightarrow$ easy, plot r vs. c_i (e.g. Fig. 1)
  - ◇ $r = k \cdot c_i^n \Rightarrow ln\, r = ln\, k + n \cdot ln\, c_i$, plot $ln\, r$ vs. $ln\, c_i$
  - ◇ $r = \frac{k \cdot p_i}{1 + K \cdot p_i} \Rightarrow \frac{p_i}{r} = \frac{1}{k} + \frac{K}{k} \cdot p_i$, plot $\frac{p_i}{r}$ vs. p_i

3.3 Integral Data Analysis

- means the suggested rate law is integrated analytically or numerically $\Rightarrow$ $n_i^*(t), c_i^*(t), p_i^*(t)$... $\Rightarrow$ comparison with experimental data ($n_i(t), c_i(t), p_i(t)$...) by means of statistical methods

$$r = \frac{1}{\nu_i}\frac{dc_i}{dt} = k \cdot c_i \;\Rightarrow\; \int_{c_i^0}^{c_i} \frac{dc_i}{c_i} = \nu_i \cdot k \int_0^t dt \;\Rightarrow\; \ln\frac{c_i}{c_i^0} = \nu_i k t \;\Rightarrow\; c_i = c_i^0 \cdot e^{\nu_i k t} \tag{28}$$

3.4 Ideal Reactors and Laboratory Reactors

- reactors for kinetic studies are often constructed to perform like one of the three ideal reactors i) batch reactor ii) PFR or iii) CSTR because these reactors are easy to analyze

- species mass balances as shown in Figure 2 are used to connect measurable quantities (concentration changes, reactant conversion, catalyst mass, flow rates) with the reaction rate $\Rightarrow$ design equation

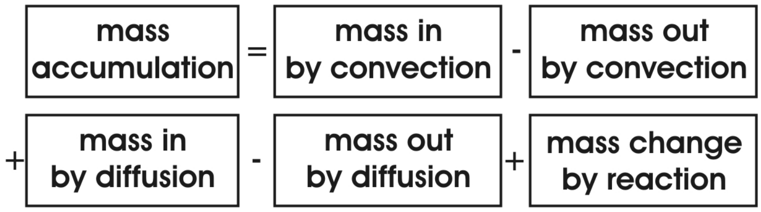

Figure 2: Typical components of a mass balance

- for isothermal reactors (ideal for kinetic studies as $r = f(T)$) there is no need to solve a heat balance, for non-isothermal reactors an analogous heat balance is solved

3.4.1 Batch Reactor

- batch reactor assumptions: constant mass, perfect mixing (no temperature and concentration gradients (Fig. 3))

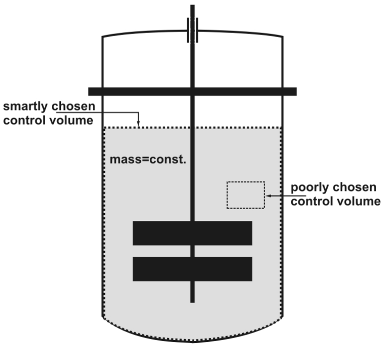

Figure 3: Schematic of a batch reactor and control volumes

- advantage: simple design (Figure 4 shows a batch reactor approach for heterogeneous catalysis studies)

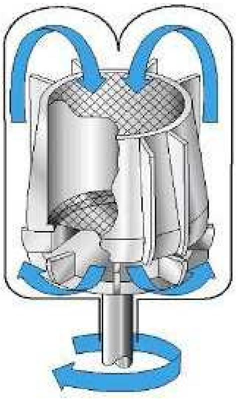

Figure 4: Spinning basket (Berty) reactor as laboratory approach of a batch reactor

- disadvantage: difficult to define $t = 0$
- online analytic (e.g. conductivity, viscosity, pressure, UV, IR) or discrete sampling (e.g. GC, HPLC, reaction quenching important!!!)
- often used for rather slow gas phase or liquid phase reactions ($t_{setup} \ll t_{reaction}$, exact definition of t_0)
- with the mass of the species m_i, the species consumption rate R_i and the molar mass of the species M_i the mass balance yields:

$$\frac{dm_i}{dt} = R_i \cdot M_i \quad [\frac{kg}{s} = \frac{mol}{s} \cdot \frac{kg}{mol}] \tag{29}$$

- note that the batch reactor operates in transient regime ($dm_i/dt \neq 0$)
- as $dm_i = dn_i \cdot M_i$ and for a reactant $dn_i = -n_i^0 dX_i$ Equation 29 transforms into
$$-n_i^0 \frac{dX_i}{dt} = R_i \quad [\frac{mol}{s} = \frac{mol}{s}] \tag{30}$$
- as the volume of the reacting fluid V (liquid or gas) is typically constant in a batch reactor, the reactant consumption can be referred to V which is practical as typically concentrations are measured
$$-\frac{n_i^0}{V}\frac{dX_i}{dt} = -c_i^0 \frac{dX_i}{dt} = -\frac{dc_i}{dt} = R_i^V \quad [\frac{mol}{m^3 s} = \frac{mol}{m^3 s}] \tag{31}$$
- alternatively, the reactant consumption rate can be referred to the catalyst mass
$$-\frac{n_i^0}{m_{cat}}\frac{dX_i}{dt} = R_i^m \quad [\frac{mol}{kg_{cat}}\frac{1}{s} = \frac{mol}{kg_{cat} \cdot s}] \tag{32}$$
- as a batch reactor experiment gives data like $X_i(t)$ one calculates the reaction rate after numerical differentiation from dX_i/dt (Equations 30-32) or uses the integrated rate law
- assigning the R_i's to concentration values is straightforward, as the concentrations are measured for each time and are the same everywhere in the reactor (ideal mixing)

3.4.2 Plug Flow Reactor (PFR)

- Figure 5 shows a schematic of a PFR reactor and typical approaches by lab reactors
- PFR assumptions: i) plug flow ii) no radial concentration gradients iii) no diffusive transport in flow direction
- to relate the reaction rate with measurable quantities a mass balance is invoked (Fig. 6)

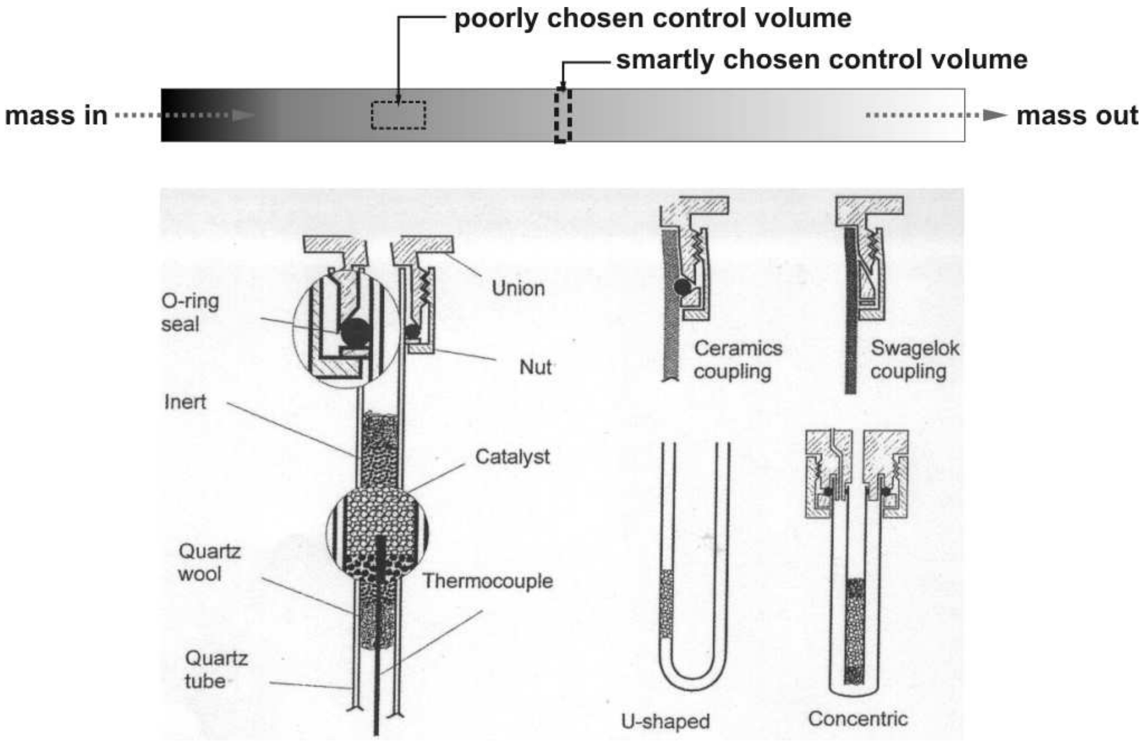

Figure 5: Schematic of a PFR and laboratory approaches

- note that in steady state, a PFR operates stationary and there is no accumulation term ($dm_i/dt = 0$)

$$d(\rho u Y_i A) = R_i \cdot M_i \tag{33}$$

- in Eqn. 33, ρ is the fluid density in kg/m^3, u is the fluid velocity in m/s, Y_i is the unitless mass fraction of species i, A is the cross section of the volume element in m^2, R_i is the production (consumption) rate of species i in mol/s and M_i is the molar mass of species i in kg/mol

- as $\rho u Y_i A$ is the mass flow rate $\dot{m}_i$ of species i in kg/s which can be expressed in terms of a molar flow rate $\dot{n}_i$, Eqn. 34 simplifies to

$$d\dot{n}_i = R_i \tag{34}$$

- as noted in Section 2.1, a catalyst mass related reaction rate is more suitable in heterogeneous catalysis than the extensive species production (consumption) rate R_i, for that reason both sides of Eqn. 34 are divided by dm_{cat},

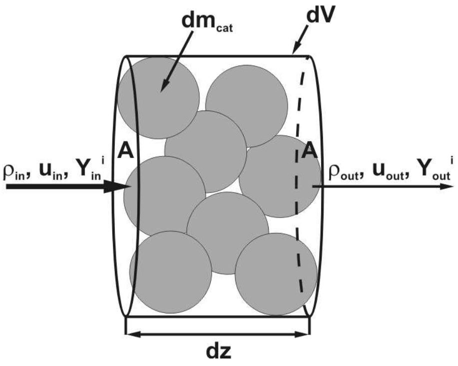

Figure 6: Mass balance over a PFR control volume with constant cross section (A =cross section in m^2, ρ =fluid density in kg/m^3, u =flow velocity in m/s, Y_i =mass fraction of species i, dz =length of control volume in m, dV = volume of control volume in m^3, dm_{cat} = catalyst mass in control volume in kg_{cat})

the differential catalyst mass in the reactor volume dV

$$\frac{d\dot{n}_i}{dm_{cat}} = R_i^{m_{cat}} \tag{35}$$

- in practice the conversion X_i of a reactant is measured and $d\dot{n}_i$ is expressed as $d\dot{n}_i = -n_i^0 \cdot dX_i$
- as n_i^0 varies from one volume element to the next it is included in the differential which leads to the so called design equation of a PFR (Eqn. 36)

$$-\frac{dX_i}{d\left(\frac{m_{cat}}{n_i^0}\right)} = R_i^{m_{cat}} \tag{36}$$

- note the similarity between Eqn. 32 and Eqn. 36
- in a PFR the time t is replaced by a contact time m_{cat}/n_i^0
- in a typical flow reactor experiment, X_i is measured at the reactor outlet and plotted against m_{cat}/n_i^0
- in principle, $X_i = f(m_{cat}/n_i^0)$ can be differentiated to determine $R_i^{m_{cat}}$, but this gives only a mean reaction rate because the reactant concentrations vary along the catalyst bed (in contrast to a batch reactor where the concentrations are everywhere the same)

- to assign a reaction rate $R_i^{m_{cat}}$ to a concentration values the flow reactor is typically operated differentially, i.e. only a small conversion ($X_i < 0.1$) is realized and Eqn. 36 turns into Eqn. 37 which allows to determine and assign the reaction rate directly

$$\frac{X_i}{\left(\frac{m_{cat}}{n_i^{in}}\right)} = -R_i^{m_{cat}} \tag{37}$$

- the lowest possible X_i is determined by the analytical precision (typically $X_i \leq 0.1$)
- disadvantage of differential reactor operation: the concentration of intermediate products are very low and can often not be measured therefore subsequent reactions of intermediate products can not be followed
- solution 1: addition of the reaction intermediates to the feed stream (Fig. 7)

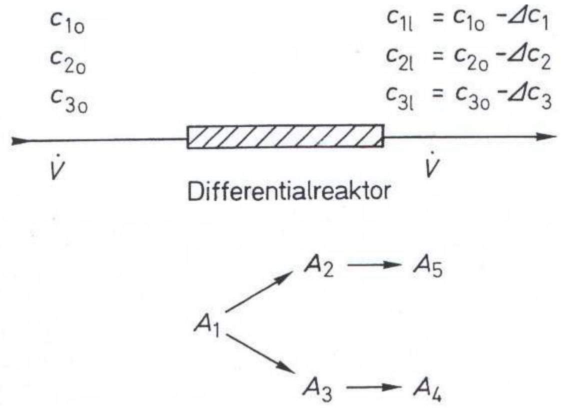

Figure 7: Addition of reaction intermediates to the feed stream of a differentially operated flow reactor (adopted from [1])

- solution 2: staged reactor (stage 1 integral, stage 2 differential, Fig. 8)
- solution 3: spatially resolved probing (Fig. 9 schematic, in practice 9)

3.4.3 Continously Stirred Tank Reactor (CSTR)

- laboratory reactors that approach the ideal **C**ontinuously **S**tirred **T**ank **R**eactor (CSTR) are besides tubular flow reactors very valuable for kinetic studies in

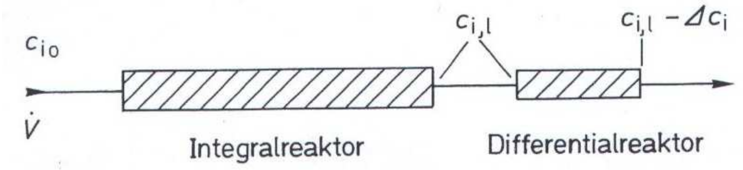

Figure 8: Integral flow reactor as input for a differential flow reactor

heterogeneous catalysis

- CSTR assumption: perfect mixing → the concentration of a species is everywhere the same in the reactor
- Figure 12 shows some design ideas for heterogeneous catalysis applications
- the relation between reaction rate and measurable quantities is again obtained from a mass balance
- we consider an isothermal CSTR in steady state ($dm_i/dt = 0$), the $\dot{m}$'s are mass flow rates in kg/s

$$\dot{m}_{total}(Y_i^{out} - Y_i^{in}) = R_i \cdot M_i \tag{38}$$

$$\dot{m}_i^{out} - \dot{m}_i^{in} = R_i \cdot M_i \tag{39}$$

$$\dot{n}_i^{out} - \dot{n}_i^{in} = R_i \tag{40}$$

$$-\dot{n}_i^{in} X_i = R_i \tag{41}$$

$$\frac{-\dot{n}_i^{in} X_i}{m_{cat}} = \frac{R_i}{m_{cat}} = R_i^{m_{cat}} \tag{42}$$

$$\frac{X_i}{\left(\frac{m_{cat}}{n_k^0}\right)} = -R_i^{m_{cat}} \tag{43}$$

- Equation 43 shows that in a CSTR, in contrast to batch reactor and PFR, the reaction rate can be measured at arbitrary large conversions X_i

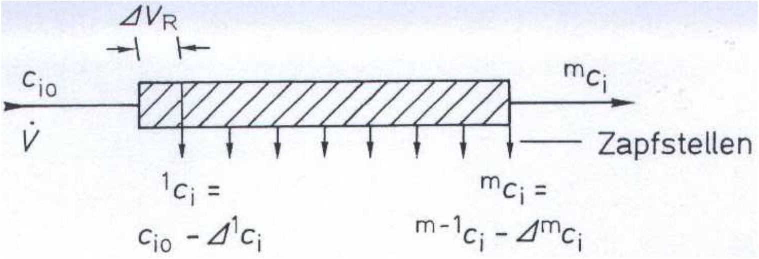

Figure 9: Schematic of a flow reactor with spatial probing

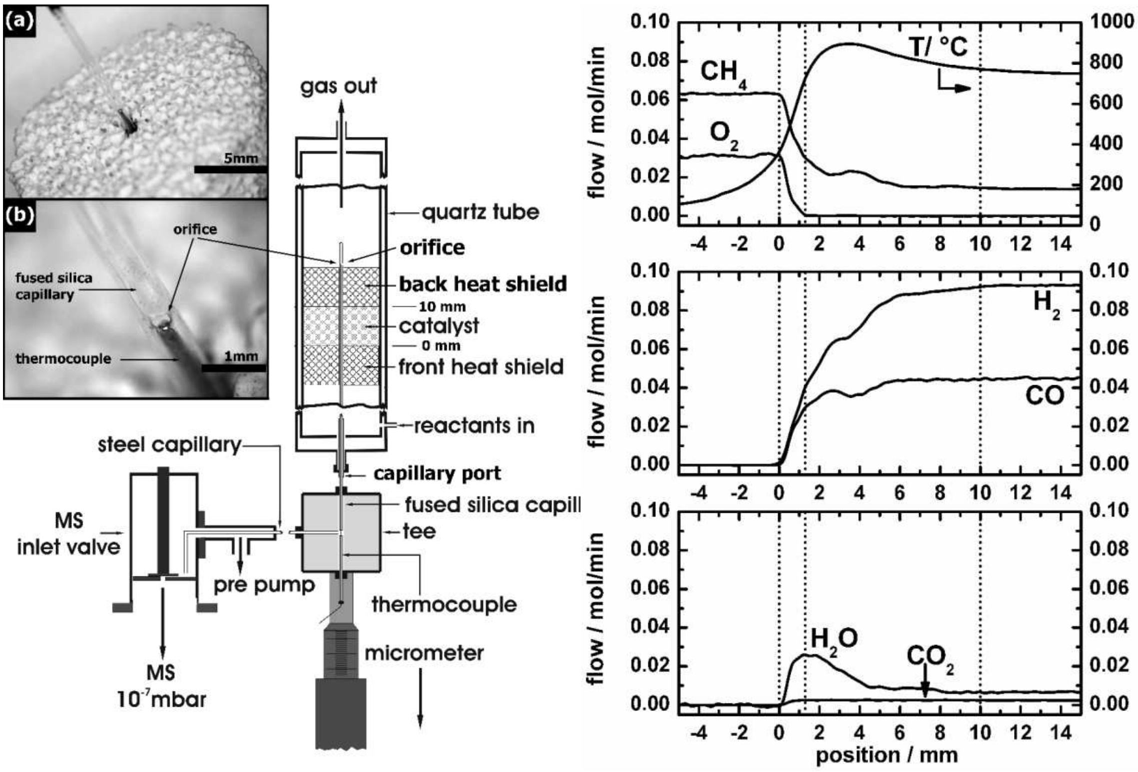

Figure 10: Spatial probing during methane oxidation on Rh [2]

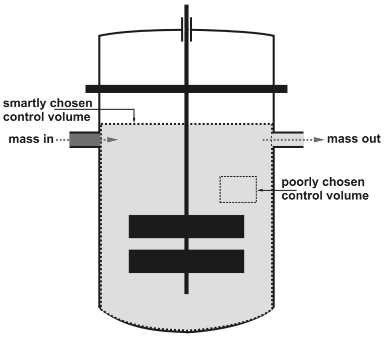

Figure 11: Schematic of a CSTR and control volumes

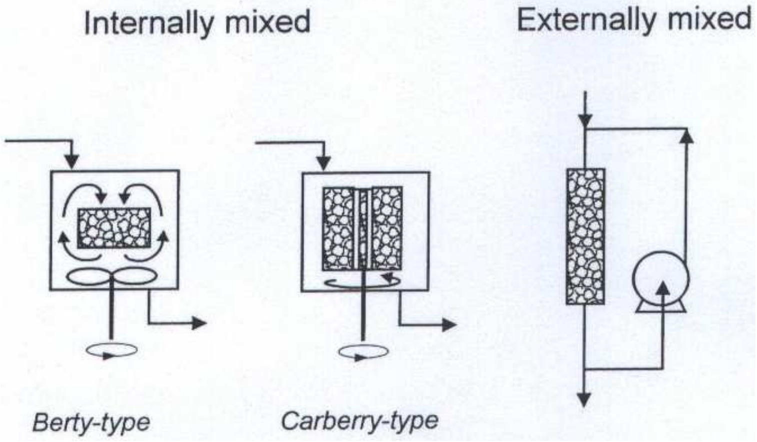

Figure 12: Schematics of CSTR's for heterogeneous catalysis applications, adopted from [3]

4 Impact of Transport on Kinetic Measurements

- in a heterogeneous system consisting of two or more phases where a component from one phase reacts in or on the other phase, physical transport processes (mass, heat, momentum) become important
- in industrial reactors reaction rates are maintained as high as possible and heat and mass transport effects are normal → this is not a problem for reactor design as transport and kinetics can be combined in a design equation
- the opposite is not true → kinetic rate equations can never be extracted from data obtained under (significant) influence of heat and mass transport
- for this reason origin and nature of transport processes need to be clear

to the experimenter and the absence of transport effects has to be verified before reporting any kinetic data

- Figure 13 illustrates how inter- and intraphase concentration and temperature gradients occur because of the finite rate of transport processes

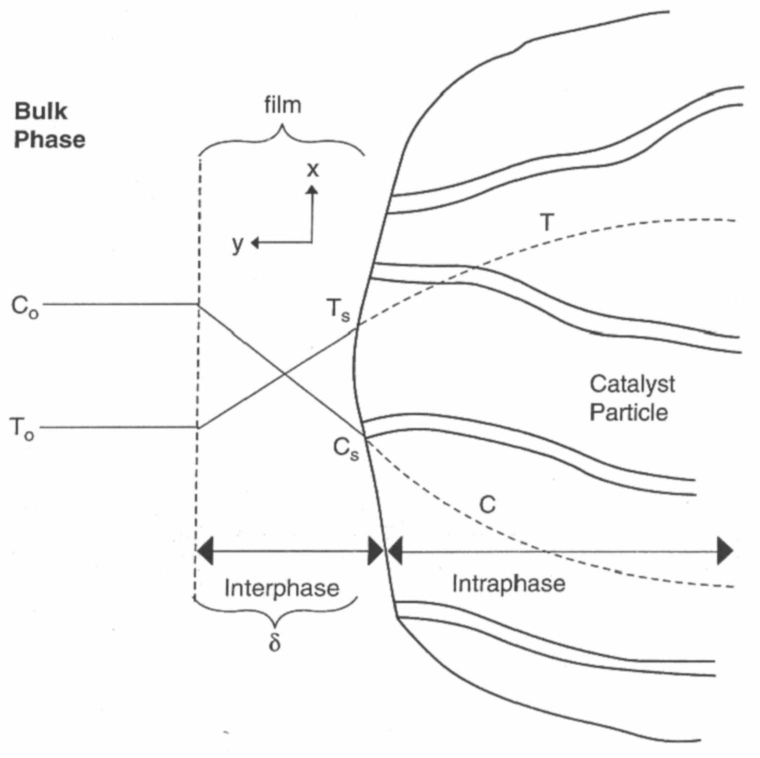

Figure 13: Concentration and temperature gradients from the bulk gas phase through a stagnant film of thickness δ to a particle surface and then through the pores of the catalyst particle (exothermic reaction assumed, adopted from [4])

- in steady state, the rates by which mass and heat are transported between the catalytic surface and the bulk fluid phase must equal the rates of mass and heat generation by the chemical reaction
- with k_g being a gas phase mass transport coefficient in m/s, a the external interphase area per unit volume in $m^2/m^3 = m^{-1}$, C_0 and C_s the bulk and surface concentrations respectively in mol/m^3, R the effective reaction rate in $mol \cdot m^{-3} \cdot s^{-1}$, k the reaction rate constant in $s^-1 \cdot (m^3 \cdot mole^{-1})^{n-1}$, n the unitless reaction order, h the heat transport coefficient in $J \cdot s^{-1} \cdot m^{-2} \cdot K^{-1}$,

T_0 and T_s the bulk and surface temperature respectively in K and ΔH the heat of reaction in $J \cdot mol^{-1}$ the following balances are obtained

$$k_g \cdot a \cdot (C_0 - C_s) = R = k \cdot C_s^n \tag{44}$$

$$h \cdot a \cdot (T_s - T_0) = -\Delta_r H \cdot R \tag{45}$$

- the reaction rate constant at the surface k_s differs of course from the reaction rate constant under bulk gas phase conditions because the ratio of surface and gas temperature $t = T_s/T_0 \neq 1$

$$k_s = k_0 \cdot exp\left[-\frac{E_a}{RT_0}\left(\frac{1}{t} - 1\right)\right] \tag{46}$$

- in the following we will have a look first at interphase mass transport (heat transport analogous) and then at the intraphase mass transport (heat transport analogous) and their consequences for the reaction rate and kinetic measurements, secondly we will discuss experimental and numerical criteria to verify presence or absence of transport effects and finally we will discuss experimental means to minimize these effects

4.1 Interphase and Intraphase Mass Transport

4.1.1 Interphase Mass Transport Coefficient

- a mass balance on the external particle-gas phase boundary layer (cp. Fig. 13) supplies a functional relationship how the species concentration varies across the external boundary layer (x axial flow direction in m, y radial flow direction in m, u flow velocity in x direction in m/s, v flow velocity in y direction in m/s, D diffusion coefficient in m^2/s)

$$u\frac{\partial C}{\partial x} + v\frac{\partial C}{\partial y} = D\left(\frac{\partial^2 C}{\partial y^2} + \frac{\partial^2 C}{\partial x^2}\right) \tag{47}$$

- neglecting convection and diffusion in flow direction x yields

$$\frac{d^2 C}{dy^2} = 0 \tag{48}$$

- this homogeneous second order ODE can be solved by finding the roots of the auxiliary equation obtained by substitution

$$C = Ae^{\lambda y} \Rightarrow \frac{d^2C}{dy^2} = \lambda^2 Ae^{\lambda y} \Rightarrow \lambda^2 = 0 \Rightarrow \lambda_1 = 0, \lambda_2 = 0 \tag{49}$$

- as the roots of the auxiliary equation are equal, we must find an additional linearly independent solution of the one already found (e^{0y})⇒ a smart guess is ye^{0y}

- the solution of the homogeneous ODE (48), the so called complementary function, is obtained by the linear superposition of the two individual solutions

$$C(y) = const_1 + const_2 \cdot y \tag{50}$$

- by using two boundary physical boundary conditions: 1) at $y = \delta \ \rightarrow C = C_0$ and 2) at $y = 0 \ \rightarrow C = C_s$ (see Fig. 13), the two constants of integration can be determined

- integration yields a linear decrease of C in the stagnant film (cp. Fig. 13):

$$C = (C_0 - C_s)\frac{y}{\delta} + C_s \tag{51}$$

- the phenomenological transport coefficient k_g is analytically defined as the flux of molecules through the film surface $(mol \cdot m^{-2} \cdot s^{-1})$ divided by the driving force

$$k_g = \frac{diffusive\ flux}{driving\ force} = \frac{D\frac{dC}{dy}|_{y=\delta}}{C_0 - C_s} = \frac{D}{\delta} \tag{52}$$

- Eqn. 52 tells you that you can increase film mass transport by decreasing δ, i.e. by increasing the flow rate (deeper discussion in Section 4.2), you can not do much about D as it is an inherent property of your gas mixture

4.1.2 Intraphase Mass Transport Coefficient

- inside the pores of the catalyst grain, diffusion is the main transport mechanism but now diffusion and reaction occur in parallel → the intraphase continuity equation results to

$$D\frac{d^2C}{dy^2} = R \tag{53}$$

- because D depends in a complicated way on porosity and tortuosity, a physical interpretation of k_g inside the catalyst pores is much more complicated and beyond the scope of this handout

4.1.3 Interphase Diffusion and Reaction

- under isothermal steady-state conditions, interphase mass transport and the surface reaction rate equal (here first order reaction for simplicity), the concentration at the surface C_s can be expressed in terms of bulk conditions and mass transport

$$k_g \cdot a \cdot (C_0 - C_s) = R = kC_s \;\Rightarrow\; C_s = \frac{C_0}{1 + \frac{k}{k_g a}} = \frac{C_0}{1 + Da_0} \tag{54}$$

- Da_0 is a so called Damköhler number, the ratio of surface chemical reaction rate to bulk mass transport
- it is instructive to compare the effective, experimentally observed reaction rate R with R_0, the rate without mass transport resistance, leading to the external effectiveness $\bar{\eta} = R/R_0$
- for $n = 1$

$$\bar{\eta} = R/R_0 = \frac{kC_0}{1 + Da_0}\frac{1}{kC_0} = \frac{1}{1 + Da_0} \tag{55}$$

- for $n = 1/2$

$$\bar{\eta} = R/R_0 = \sqrt{\frac{2 + Da_0^2}{2}\left[1 - \sqrt{1 - \frac{4}{(2 + Da_0^2)^2}}\right]} \tag{56}$$

- for $n = 2$

$$\bar{\eta} = R/R_0 = \left[\frac{1}{2Da}(\sqrt{1 + 4Da} - 1)\right] \tag{57}$$

- where always

$$Da_0 = \frac{kC_0^{n-1}}{k_g a} = \frac{chemical\ reaction\ rate}{mass\ transport\ rate} \tag{58}$$

- Fig. 14 shows the $\bar{\eta}$=f(Da_0) relationship for reactions of different orders $\Rightarrow$ you can see that i) the impact of interphase transport limitation increases with the reaction order and ii) that for negative reaction orders (reactant inhibition) $\bar{\eta}$ increases unity

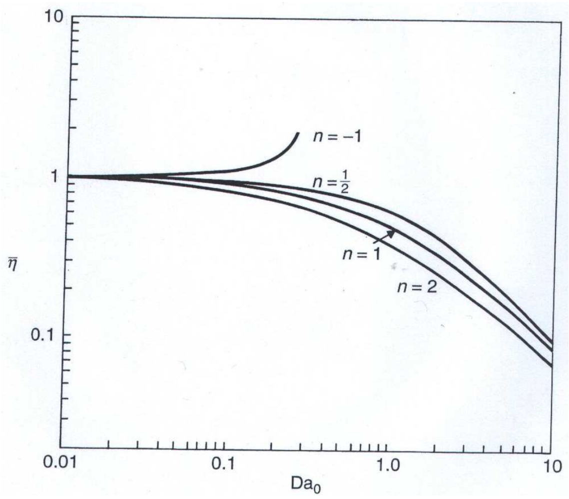

Figure 14: Isothermal external catalytic effectiveness for reaction order n [4])

- if we knew the Damkoehler number we could calculate $\bar{\eta}$ and assess the importance of interphase mass transport on our observed reaction rate $\rightarrow$ problem: k and hence Da are usually not known $\rightarrow$ we have to find a relation between $\bar{\eta}$ and something we can measure
- because the measurable reaction rate $R = \bar{\eta} k C_0 = \bar{k} C_0$ and $\bar{k} = \bar{\eta} k$ we have

$$\frac{\bar{k}}{k_g a} = \bar{\eta}\frac{k}{k_g a} = \bar{\eta} Da = \frac{R}{k_g a C_0} \tag{59}$$

- in contrast to Da, $\bar{\eta}Da$ is measurable (we measure R, know C_0, k_g comes out of a transport correlation e.g. for packed beds and a can be calculated from the particle geomtrey)
- what we need is a relationship between $\bar{\eta}$ and $\bar{\eta}Da$, this can be obtained from a heat balance
- in general $T_0 \neq T_s$, $C_0 \neq C_s$ and $k_0 \neq k_s$

$$\bar{\eta} = \frac{k_s}{k_0}\left(\frac{C_s}{C_0}\right)^n \tag{60}$$

- from Eqn. 44 we know that

$$\frac{C_s}{C_0} = 1 - \frac{R}{k_g a C_0} \tag{61}$$

- hence, from Eqn. 59

$$\frac{C_s}{C_0} = 1 - \bar{\eta} Da \tag{62}$$

- and our relationship results to Eqn. 63, which is graphically displayed in Figure 15

$$\bar{\eta} = \frac{k_s}{k_0}(1 - \bar{\eta} Da)^n \tag{63}$$

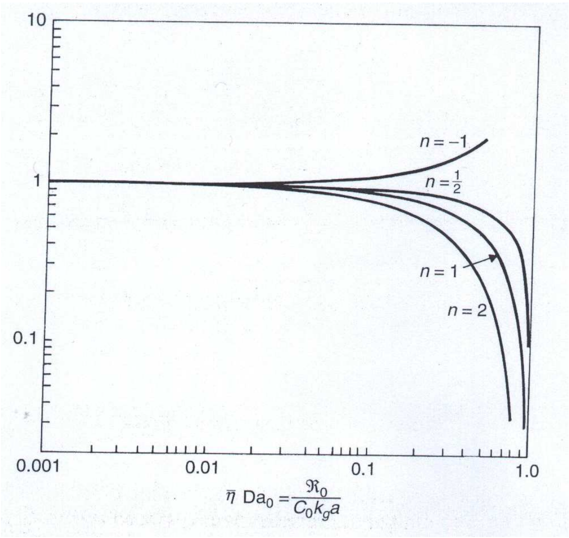

Figure 15: Isothermal external catalytic effectiveness in terms of observables for order n [4])

- for nonisothermal systems ($t = T_s/T_0$ and $\varepsilon_0 = E/RT_0$)

$$\frac{k_s}{k_0} = e^{-\frac{E}{R}\left(\frac{1}{T_s} - \frac{1}{T_0}\right)} = e^{-\frac{E}{RT_0}\left(\frac{1}{t} - 1\right)} = e^{-\varepsilon_0\left(\frac{1}{t} - 1\right)} \tag{64}$$

- from Eqn. 45 we get

$$t = \frac{T_s}{T_0} = 1 - \frac{\Delta H R}{haT_0} = 1 + \left(\frac{-\Delta H k_g a C_0}{haT_0}\right)\left(\frac{R}{k_g a C_0}\right) = 1 + \bar{\beta} \cdot \bar{\eta} Da \tag{65}$$

- inserting Eqn. 65 into Eqn. 64 and Eqn. 63 yields Eqn. 66, graphically shown in Figure 16

$$\bar{\eta} = (1 - \bar{\eta} Da)^n e^{-\varepsilon_0 \left(\frac{-\bar{\beta} \cdot \bar{\eta} Da}{1 + \bar{\beta} \cdot \bar{\eta} Da} \right)} \tag{66}$$

4.1.4 Intraphase Diffusion and Reaction

- in the pores of the catalyst particle, diffusion and reaction occur in parallel in contrast to interphase transport where diffusion and reaction occur in series $\Rightarrow$ the deeper the catalytic sites are inside the particle the harder they are accessible and the lesser they contribute to the overall reaction rate (Fig. 17)

- at steady state the moles of a reactant species diffusing into a differential spherical volume element minus the moles diffusing out of the differential spherical volume element must equal the moles converted by the chemical reaction

$$d(flux \cdot area) = RdV \left[\frac{mol}{m^2 s} \cdot m^2 = \frac{mol}{m^3 s} \cdot m^3 \right] \tag{67}$$

$$\frac{d(flux \cdot area)}{dV} = R \Rightarrow \frac{d\left[-D \left(\frac{dC}{dr} \right) 4\pi r^2 \right]}{4\pi r^2 dr} = -kC^n \tag{68}$$

- this leads to the following differential equation

$$D \left(\frac{d^2 C}{dr^2} + \frac{2}{r} \frac{dC}{dr} \right) = kC^n \tag{69}$$

- by introducing $f = C/C_s$ and $\rho = r/R_p$, Eqn. 69 is made dimensionless leading to

$$\frac{d^2 f}{d\rho^2} + \frac{2}{\rho} \frac{df}{d\rho} = \left(\frac{R_p^2 k C_s^{n-1}}{D} \right) f^n \tag{70}$$

- the term in parentheses on the rhs of Eqn. 70 is the square of the Thiele Modulus ϕ, which measures the ration of chemical reaction rate relative to the intraphase (pore) diffusion rate

$$\phi^2 = \frac{R_p^2 k C_s^{n-1}}{D} \tag{71}$$

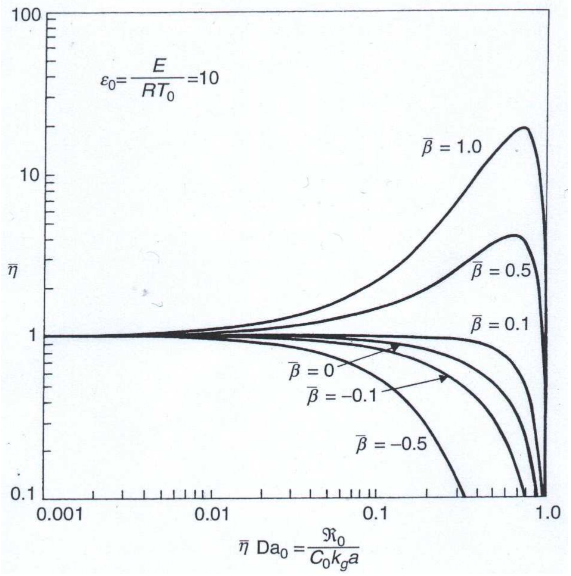

Figure 16: External nonisothermal effectiveness $\bar{\eta}$ vs. observables ($n = 1$, $\varepsilon_0 = 10$) [4])

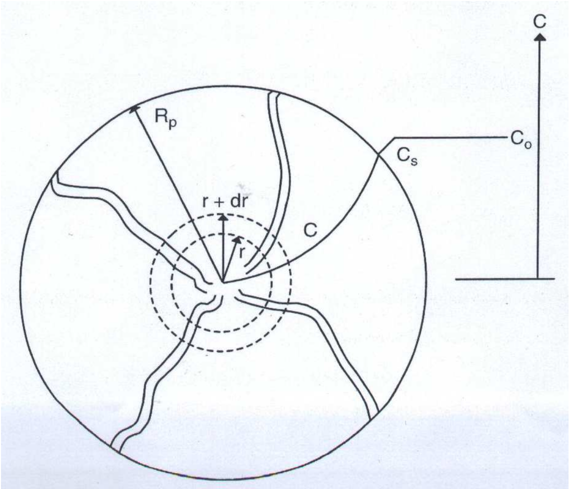

Figure 17: Concentration profile of a reactant from the bulk gas phase (C_0) to the particle surface (C_s) to the center of a catalyst particle with radius R_p [4]

- Eqn. 70 can be solved for reactions of different order using the boundary conditions $df/d\rho = 0$ at $\rho = 0$ and $f = 1$ at $\rho = 1$

- for a first order reaction $n = 1$ the solution reads to

$$f = \frac{C}{C_s} = \frac{sinh\,\phi\rho}{\rho \cdot sinh\,\phi} \tag{72}$$

- now, an isothermal effectiveness factor can be defined comparing the observed rate with transport limitations to the rate without transport limitations ($C = C_s$ throughout the catalyst particle)

$$\eta = \frac{1}{kC_sV}\int_0^V kCdV = \frac{4\pi}{(4/3)\pi R^3 C_s}\int_0^R Cr^2dr \tag{73}$$

- integration yields

$$\eta = \frac{3}{\phi}\left(\frac{1}{tanh\,\phi} - \frac{1}{\phi}\right) = \frac{3}{\phi^2}\left(\phi coth\,\phi - 1\right) \tag{74}$$

- the hyperbolic sine $sinh(x)$, the hyperbolic cosine $cosh(x)$ and the hyperbolic tangent $tanh(x)$ arise frequently in science and engineering problems

- the hyperbolic functions are related to the exponential functions as follows, a graph is shown in Figure 18

$$sinh(x) = \frac{1}{2}\left(e^x - e^{-x}\right) \tag{75}$$

$$cosh(x) = \frac{1}{2}\left(e^x + e^{-x}\right) \tag{76}$$

$$tanh(x) = \frac{(e^x - e^{-x})}{(e^x + e^{-x})} \tag{77}$$

- Figure 19 shows the $\eta = f(\phi)$ relationship for different reaction orders $n \Rightarrow$ note that similar to film transport, the impact of pore transport increases with reaction order

- for large ϕ, η approaches $3/\phi$

- with this simple relationship we can now explore the impact of pore transport on experimentally measured kinetic parameters

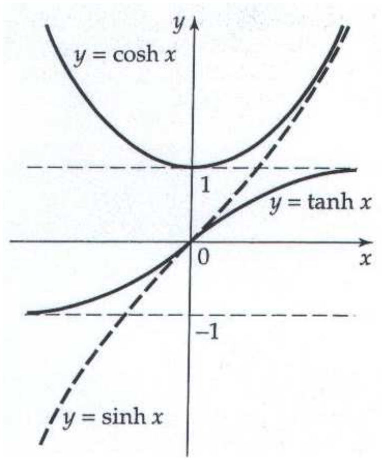

Figure 18: Shapes of the hyperbolic functions $sinh(x)$, $cosh(x)$ and $tanh(x)$

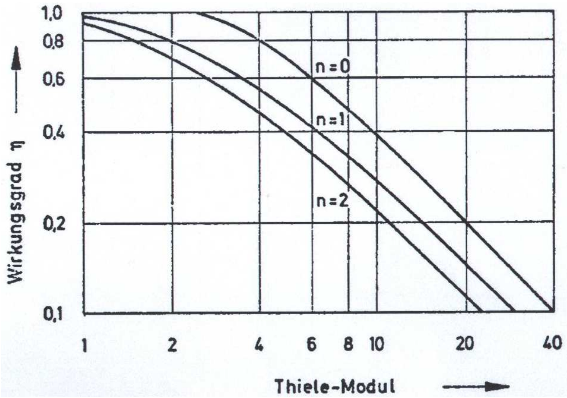

Figure 19: Dependence of η on the Thiele Modulus ϕ, adopted from [3]

4.1.5 Impact of Transport Limitations on Measured Kinetic Parameters

- lets first assume interphase (film) mass transport limitations have been removed ($C_s = C_0$) but there are strong intraphase (pore) transport limitations ($\eta \simeq 3/\phi$) $\Rightarrow$ the measured reaction rate is determined by (use of Eqn. 71)

$$R = \eta k C_0^n = \frac{3kC_0^n}{\phi} = \frac{3kC_0^n}{R_p\left(\frac{kC_0^{n-1}}{D}\right)^{1/2}} = \frac{3(kD)^{1/2}}{R_p}C_0^{(n+1)/2} = k_{meas} \cdot C_0^{n_{meas}} \tag{78}$$

- Eqn. 78 gives you already a hint how to check experimentally on intraphase mass transport limitations (make R_p smaller and see if R changes), but more importantly, it tells you how your measured reaction order n and activation energy E_a deviate from the true values

- in the regime of pore diffusion control, the measured reaction order is related to the true reaction order by

$$n_{meas} = (n+1)/2 \tag{79}$$

- because $k = k_0 \cdot exp(-E_k/RT)$ and $D = D_0 \cdot exp(-E_D/RT)$

$$(kD)^{1/2} = (k_0 D_0)^{1/2} exp^{-\frac{E_k+E_D}{2RT}} \tag{80}$$

- if you make an Arrhenius plot of your measured $ln(R)$ vs. $1/T$ you will find in case of dominating pore transport (Eqn.78)

$$ln(R) = const. - \frac{E_k + E_D}{2RT} \tag{81}$$

- and because the activation energy for diffusion is very small, much smaller than typical activation energies for catalytic reactions ($E_D << E_k$)

$$E_{meas} = \frac{E_k + E_D}{2} \approx \frac{E_k}{2} \tag{82}$$

- over the entire investigated temperature range your Arrhenius plot might actually look like Figure 20 ⇒ i) at low temperatures ($1/T$ high) chemistry is slow and you measure true reaction kinetics ($E_{meas} = E_k$), ii) if the temperature is increased ($1/T$ decreases) the reaction inside the catalyst particle speeds up and pore diffusion becomes significant ($E_{meas} \approx E_k/2$), iii) at high temperatures (small $1/T$ values) the chemistry is so fast that every incoming reactant molecule is immediately consumed at the outer layer of the catalyst particle ($C_s \rightarrow 0$) and interphase (film) transport is the slowest step ($E_{meas} \approx 0$)

4.2 Checking and Avoiding Transport Impact

- there are a number of numerical criteria in the literature to verify the absence of interphase and intraphase transport limitations (see Fig. 21 and for details [1, p.145,146 and references therein])

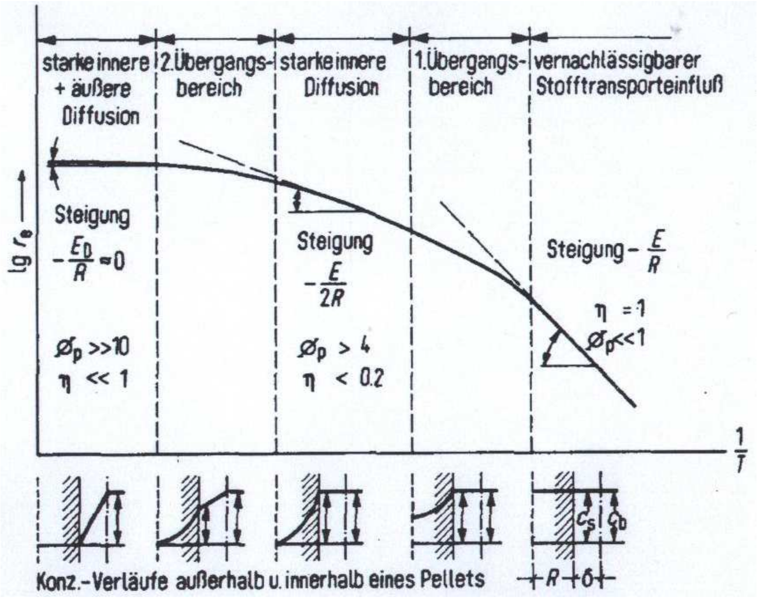

Figure 20: Change of measured activation energy by inter- and intraphase mass transport, adopted from [5]

- these numerical criteria contain the measured reaction rate, catalyst dimensions, porosity, mass and heat transport coefficient, diffusion coefficient etc.

- it is beyond the scope of this lecture to discuss these numerical criteria in detail, however, two simple experimental tests to check for interphase and intraphase transport can be devised based on the material presented in this script

- for interphase (film) mass transport we have learned that $R = kC_s = \frac{kC_0}{1+\frac{k}{k_g a}}$ (Eqn. 54) and with $k_g = D/\delta$ (Eqn. 52) we obtain

$$R = \frac{kC_0}{1 + \frac{k\delta}{Da}} \tag{83}$$

- if the R does not change by decreasing δ interphase mass transport is sufficiently fast

- δ can be decreased by i) increasing the flow rate n_i^0 in a PFR at constant $m_{cat}/n_i^0 \Rightarrow m_{cat}$ has to increase as well, ii) by increasing the internal circulation in a Batch or CSTR reactor (propeller speed) or iii) increasing the recirculation ratio in a reactor with external recirculation

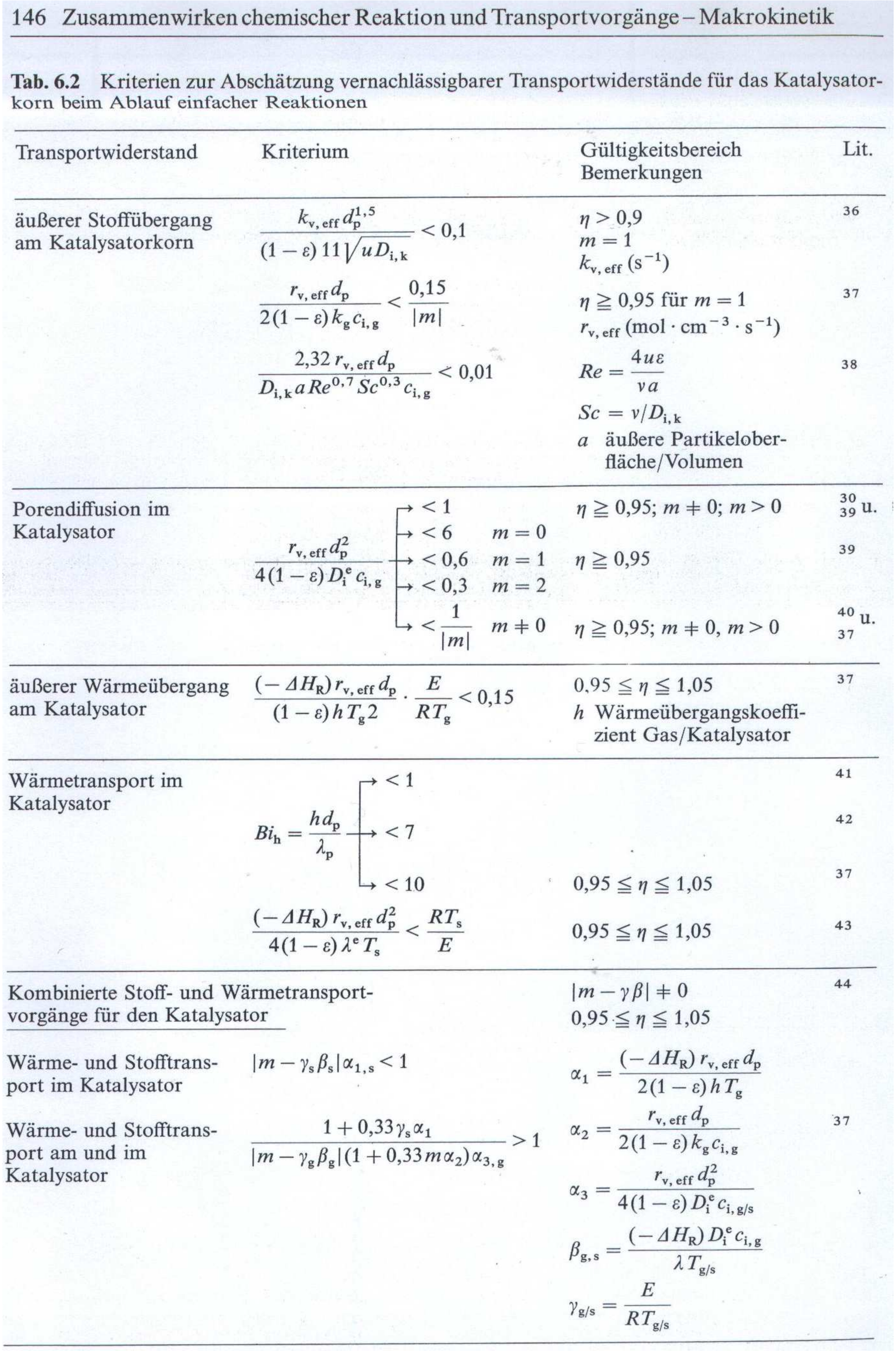

146 Zusammenwirken chemischer Reaktion und Transportvorgänge – Makrokinetik

Tab. 6.2 Kriterien zur Abschätzung vernachlässigbarer Transportwiderstände für das Katalysatorkorn beim Ablauf einfacher Reaktionen

Transportwiderstand	Kriterium	Gültigkeitsbereich Bemerkungen	Lit.
äußerer Stoffübergang am Katalysatorkorn	$\frac{k_{\mathrm{v,\,eff}}\, d_{\mathrm{p}}^{1,5}}{(1-\varepsilon)\, 11 \sqrt{u D_{\mathrm{i,\,k}}}} < 0{,}1$	$\eta > 0{,}9$ $m = 1$ $k_{\mathrm{v,\,eff}}\ (\mathrm{s}^{-1})$	36
	$\frac{r_{\mathrm{v,\,eff}}\, d_{\mathrm{p}}}{2(1-\varepsilon)\, k_{\mathrm{g}}\, c_{\mathrm{i,\,g}}} < \frac{0{,}15}{\lvert m \rvert}$	$\eta \geqq 0{,}95$ für $m = 1$ $r_{\mathrm{v,\,eff}}\ (\mathrm{mol} \cdot \mathrm{cm}^{-3} \cdot \mathrm{s}^{-1})$	37
	$\frac{2{,}32\, r_{\mathrm{v,\,eff}}\, d_{\mathrm{p}}}{D_{\mathrm{i,\,k}}\, a\, Re^{0,7}\, Sc^{0,3}\, c_{\mathrm{i,\,g}}} < 0{,}01$	$Re = \frac{4 u \varepsilon}{\nu a}$ $Sc = \nu / D_{\mathrm{i,\,k}}$ a äußere Partikeloberfläche/Volumen	38
Porendiffusion im Katalysator	$\frac{r_{\mathrm{v,\,eff}}\, d_{\mathrm{p}}^2}{4(1-\varepsilon)\, D_{\mathrm{i}}^{\mathrm{e}}\, c_{\mathrm{i,\,g}}} \rightarrow < 1$	$\eta \geqq 0{,}95;\ m \neq 0;\ m > 0$	30 u. 39
	$\rightarrow < 6 \quad m = 0$		
	$\rightarrow < 0{,}6 \quad m = 1$	$\eta \geqq 0{,}95$	39
	$\rightarrow < 0{,}3 \quad m = 2$		
	$\rightarrow < \frac{1}{\lvert m \rvert} \quad m \neq 0$	$\eta \geqq 0{,}95;\ m \neq 0,\ m > 0$	40 u. 37
äußerer Wärmeübergang am Katalysator	$\frac{(-\Delta H_{\mathrm{R}})\, r_{\mathrm{v,\,eff}}\, d_{\mathrm{p}}}{(1-\varepsilon)\, h\, T_{\mathrm{g}}\, 2} \cdot \frac{E}{R T_{\mathrm{g}}} < 0{,}15$	$0{,}95 \leqq \eta \leqq 1{,}05$ h Wärmeübergangskoeffizient Gas/Katalysator	37
Wärmetransport im Katalysator	$Bi_{\mathrm{h}} = \frac{h\, d_{\mathrm{p}}}{\lambda_{\mathrm{p}}} \rightarrow < 1$		41
	$\rightarrow < 7$		42
	$\rightarrow < 10$	$0{,}95 \leqq \eta \leqq 1{,}05$	37
	$\frac{(-\Delta H_{\mathrm{R}})\, r_{\mathrm{v,\,eff}}\, d_{\mathrm{p}}^2}{4(1-\varepsilon)\, \lambda^{\mathrm{e}}\, T_{\mathrm{s}}} < \frac{R T_{\mathrm{s}}}{E}$	$0{,}95 \leqq \eta \leqq 1{,}05$	43
Kombinierte Stoff- und Wärmetransportvorgänge für den Katalysator		$\lvert m - \gamma \beta \rvert \neq 0$ $0{,}95 \leqq \eta \leqq 1{,}05$	44
Wärme- und Stofftransport im Katalysator	$\lvert m - \gamma_{\mathrm{s}} \beta_{\mathrm{s}} \rvert\, \alpha_{1,\mathrm{s}} < 1$	$\alpha_1 = \frac{(-\Delta H_{\mathrm{R}})\, r_{\mathrm{v,\,eff}}\, d_{\mathrm{p}}}{2(1-\varepsilon)\, h\, T_{\mathrm{g}}}$	
Wärme- und Stofftransport am und im Katalysator	$\frac{1 + 0{,}33\, \gamma_{\mathrm{s}}\, \alpha_1}{\lvert m - \gamma_{\mathrm{g}} \beta_{\mathrm{g}} \rvert\, (1 + 0{,}33\, m\, \alpha_2)\, \alpha_{3,\mathrm{g}}} > 1$	$\alpha_2 = \frac{r_{\mathrm{v,\,eff}}\, d_{\mathrm{p}}}{2(1-\varepsilon)\, k_{\mathrm{g}}\, c_{\mathrm{i,\,g}}}$ $\alpha_3 = \frac{r_{\mathrm{v,\,eff}}\, d_{\mathrm{p}}^2}{4(1-\varepsilon)\, D_{\mathrm{i}}^{\mathrm{e}}\, c_{\mathrm{i,\,g/s}}}$ $\beta_{\mathrm{g,\,s}} = \frac{(-\Delta H_{\mathrm{R}})\, D_{\mathrm{i}}^{\mathrm{e}}\, c_{\mathrm{i,\,g}}}{\lambda\, T_{\mathrm{g/s}}}$ $\gamma_{\mathrm{g/s}} = \frac{E}{R T_{\mathrm{g/s}}}$	37

Figure 21: Numerical criteria to verify the absence of transport limitations for simple reactions, adopted from [1]

- Figure 22 shows the effect for the first and the last case

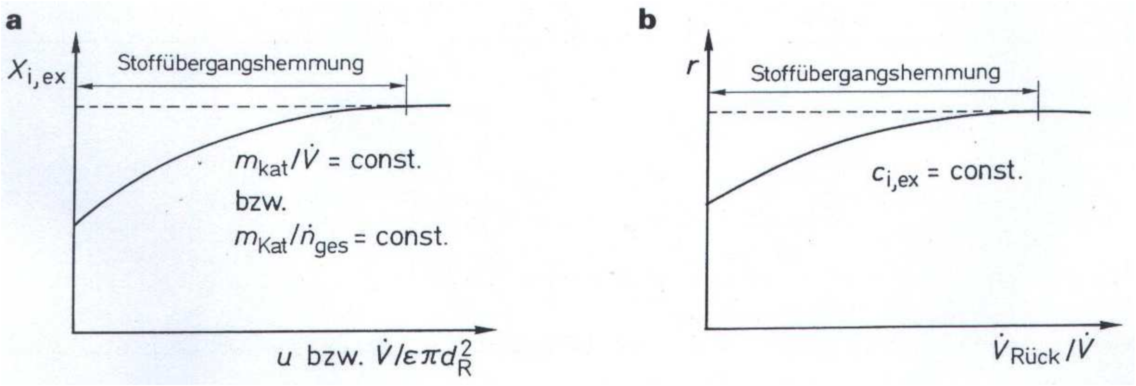

Figure 22: Experimental verification of interphase mass transport by decreasing the film thickness δ in a) PFR reactor and b) reactor with external recirculation, adopted from [1]

- if intraphase (pore) mass transport limitations are pronounced we have learned that the reaction rate depends inversely on the radius of the catalyst particle R_p

$$R = \frac{3(kD)^{1/2}}{R_p} C_0^{(n+1)/2} \tag{84}$$

- a simple experimental test to verify absence of intraphase (pore) transport limitations is to use smaller catalyst particles at constant catalyst mass $\Rightarrow$ if R increases, pore transport is slow and impacts kinetic measurements

References

[1] M. Baerns; H. Hofmann; A. Renken. *Chemische Reaktionstechnik Band 1*. Wiley-VCH, 3rd edition, 1999.

[2] R. Horn; K. A. Williams; N. J. Degenstein; L. D. Schmidt. Mechanism of h_2 and co formation in the catalytic partial oxidation of ch_4 on rh probed by steady-state spatial profiles and spatially resolved transients. *Chem. Eng. Sci.*, 62:1298–1307, 2007.

[3] F. Kapteijn; J. A. Moulijn. *Handbook of Heterogeneous Catalysis*, volume 3, chapter 6, pages 1189–1261. Wiley-VCH, 1997.

[4] M. A. Vannice. *Kinetics of Catalytic Reactions*. Springer, 1st edition, 2005.

[5] G. Emig. Skriptum zur kernvorlesung reaktionstechnik. online - not available anymore, 1999.